Processing of incident-neutron sub-library from ENDF/B-VII.1, JENDL-4.0 and JEFF-3.1.1

M.P.W. Chin, A. Ferrari, V. Vlachoudis
CERN (European Organization for Nuclear Research), CH-1211 Geneva, Switzerland

Abstract
FLUKA has so far achieved fully correlated/analog simulation for almost all projectile-target-energy combinations. This work reports some efforts in extending correlated transport to cover the <20 MeV neutron range, which is presently given, for the most part, multigroup treatment. The dynamics of correlated and multigroup transport will be demonstrated in the form of a sample history. Some issues arising from the processing of evaluated incident-neutron sub-libraries, using PREPRO and NJOY, will be presented. The representation of angular distribution of neutron elastic scatter will be discussed, with an attempt parameterize Legendre coefficients.

1 Correlated versus uncorrelated radiation transport

FLUKA [1,2] is capable of correlated simulation of all projectile-target combinations from eV to TeV – except for some cases where the neutron is below 20 MeV. In fact, even for low-energy (<20MeV) neutrons, correlated pointwise simulation is already available for selected channels. Wide-scale implementation of correlated pointwise transport is in progress; some aspects will be reported in Section 2.

In correlated/analog simulation, energy, momentum, A and Z are fully conserved at each collision – even before averaging over multiple samples; each secondary particle in the cascade fits a unique place in a *family tree*; the relation between every particle is uniquely defined.

Listing 2 is a sample history following a 20.1 MeV neutron in ^{10}B. FLUKA seamlessly switches to multigroup (non-correlated) transport when the neutron goes below 20.0 MeV (line 4). Before line 4, the neutron energy is exactly resolved (eg. 20.1 MeV at line 2). Once multigroup transport takes effect, however, the neutron energy becomes known between group-specific limits (eg. 19.6 and 20.0 MeV at line 4). The α produced at line 5 later collides, $\alpha +^{11} B \rightarrow^{14} C + p + \gamma$ (line 7), conserving A and Z. $^{10}B(n,\alpha)^{7}Li$ capture, the principle behind typical neutron detection, shielding and therapy, takes place in line 37; momentum and energy strictly conserved, FLUKA switches back to fully correlated transport. The accompanying 0.477 MeV γ, emitted explicitly as a sharp line, later interacts (line 39).

Estimation of integrated quantities (eg. dose and fluence) typically does not require correlation. Multigroup treatment is therefore a common technique in neutron transport; it offers greater details than the discrete ordinate technique. In fact, there are widely-used codes, where pointwise transport has been available, that are uncorrelated by design and philosophy. Correlated transport is optional, and challenging, in terms of code development.

There are applications which may be sensitive to the lack of correlation (eg. single event upsets and tissue equivalent proportional counters). Hence the importance of overcoming current exceptions where full correlation is absent in FLUKA. A point to note is that fully-correlated transport does not necessarily imply long run-times, as variance reduction techniques are always available.

2 Processing evaluated libraries: from ENDF to PENDF

A preliminary step towards implementing correlated low-energy neutron transport is to draw necessary data from evaluated libraries. Evaluated data in its raw form (ENDF [3]) are not readily usable feeds. Pointwise (PENDF) data may be obtained by processing ENDF using PREPRO [4] or NJOY [5].

	MeV	ns	cm
−>n	2.01000000000 e+01	0.000000000 e+00	0.000000000 e+00
∗elastic	2.01000000000 e+01	1.355819720 e−02	8.275412706 e−02
|−recoil	1.71238952200 e−01	1.355819720 e−02	8.275412706 e−02
∗multig	1.96e+01_2.00e+01	2.396900352 e−01	1.453660049 e+00
−>2004	1.34750201500 e+01	2.396900352 e−01	1.453660049 e+00
|−step	2.17511493300 e+00	2.406580743 e−01	1.454112416 e+00
∗inelast	1.12999052200 e+01	2.406580743 e−01	1.454112416 e+00
−>6014	3.40657375900 e+00	2.406580743 e−01	1.454112416 e+00
|−step	3.40657375900 e+00	2.409063336 e−01	1.454126090 e+00
−>g	6.87132216600 e+00	2.406580743 e−01	1.454112416 e+00
∗Compton	6.87132216600 e+00	8.904385034 e−01	1.894811647 e+01
−>e−	6.29794025900 e+00	8.904385034 e−01	1.894811647 e+01
|−step	1.35455567600 e+00	9.025436869 e−01	1.929863451 e+01
|−step	9.07954558600 e−01	9.120798329 e−01	1.955831973 e+01
|−step	6.79128727100 e−01	9.198851972 e−01	1.966286332 e+01
|−step	6.33787894500 e−01	9.263898577 e−01	1.964319996 e+01
|−step	4.61618544000 e−01	9.316649092 e−01	1.954360203 e+01
|−step	3.72014477900 e−01	9.360452237 e−01	1.941729579 e+01
|−step	6.40817203300 e−01	9.397475699 e−01	1.931408822 e+01
|−step	1.91924358900 e−01	9.422203163 e−01	1.925041108 e+01
|−step	1.86279218600 e−01	9.441378768 e−01	1.920272774 e+01
∗Compton	5.73381906500 e−01	9.539757657 e−01	1.948346534 e+01
−>e−	1.61188100300 e−01	9.539757657 e−01	1.948346534 e+01
∗Compton	4.12193806200 e−01	1.034231071 e+00	2.145125437 e+01
−>e−	5.79735126300 e−02	1.034231071 e+00	2.145125437 e+01
∗Compton	3.54220293600 e−01	1.122923115 e+00	2.256353592 e+01
−>e−	1.10342679600 e−01	1.122923115 e+00	2.256353592 e+01
−>p	1.80576864000 e+00	2.406580743 e−01	1.454112416 e+00
|−step	1.80576864000 e+00	2.441490229 e−01	1.456045267 e+00
−>3007	8.76983895000 e+00	2.396900352 e−01	1.453660049 e+00
|−step	8.76983895000 e+00	2.405904497 e−01	1.454209451 e+00
|−recoil	3.64007707700 e+00	2.396900352 e−01	1.453660049 e+00
∗multig	1.92e+01_1.96e+01	4.332574626 e−01	2.583124903 e+00
|−recoil	3.57532332400 e+00	4.332574626 e−01	2.583124903 e+00
∗multig	8.39e+00_8.61e+00	2.335985032 e+00	9.579404378 e+00
|−recoil	1.93476781700 e+00	2.335985032 e+00	9.579404378 e+00
∗multig	8.19e+00_8.39e+00	2.566380818 e+00	1.043058092 e+01
−>g	4.77610000000 e−01	2.566380818 e+00	1.043058092 e+01
∗Compton	4.77610000000 e−01	2.705250677 e+00	7.496920262 e+00
−>e−	2.03933671000 e−01	2.705250677 e+00	7.496920262 e+00
−>2004	7.93477174700 e+00	2.566380818 e+00	1.043058092 e+01
|−step	7.93477174700 e+00	2.570277887 e+00	1.043239819 e+01
−>3007	3.14540634600 e+00	2.566380818 e+00	1.043058092 e+01
|−step	3.14540634600 e+00	2.566780987 e+00	1.043058384 e+01
|−recoil	1.88226392500 e+00	2.566380818 e+00	1.043058092 e+01

Listing 1: Sample cascade from a slowing-down neutron in FLUKA. Time and distance are given with respect to source origin. The energy column shows 1) the kinetic energy at collision (arrows) or production (stars); 2) the kinetic energy range when multigroup (multig) treatment is in effect; 3) energy deposition for steps and recoils. Ions are represented in ZA notation. Indents denote the nth particle generation.

Fig. 1 shows the minimum cross section for different materials and reaction types. Data have been extracted from ENDF/B.VII.1 and JENDL-4.0. This is of particular interest given that PREPRO takes as input parameter a threshold in barns, below which cross sections would be copied verbatim. The default threshold is 1×10^{-10} barns, whereas the minimum cross sections do go well below this value (Fig. 1).

Fig. 2 shows the $(n, n'\alpha)$ cross section for ^{94}Nb after linearization and resonance reconstruction by NJOY and PREPRO. In this case it is easy to recognize which is correct. Plotted on a log-linear scale, with the ENDF file clearly specifying the interpolation scheme as log-linear, lines joining adjacent points should be straight. The disagreement at low energies is due to the above-mentioned threshold in PREPRO input. Lowering the threshold would solve the problem. The author of PREPRO, however, maintains that the threshold should be kept at 1×10^{-10} barns to avoid potential problems in the presence of resonance.

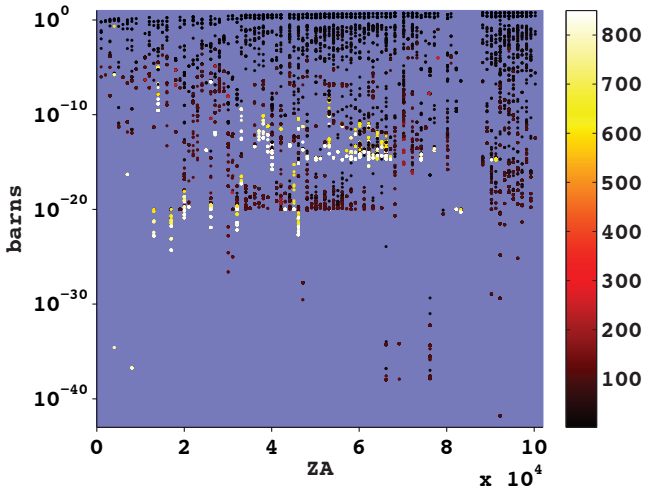

Fig. 1: The minimum cross section for various ZA available from the incident-neutron sub-library of ENDF/B-VII.1 and JENDL-4.0. Colour scales from low MT (dark) to high MT (bright).

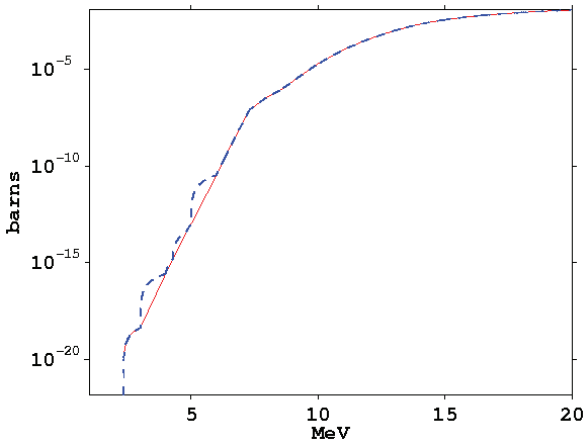

Fig. 2: Cross section after linearization and resonance reconstruction using PREPRO with default settings (dashed line) and NJOY (full line): Nb-94 MT=22.

Whereas either PREPRO or NJOY could have accomplished the task, we used both, as a tangential quality assurance exercise to spot vulnerabilities requiring attention. The amount of data calls for a balance between automation and human intervention, to address the risk of missing details (due to over-automation) and making mistakes (due to unnecessarily manual handling).

3 Angular distribution of neutron elastic scattering

Angular distribution (MF=4) of elastic scattering (MT=2) may be represented in several forms: 1) a flag indicating purely isotropic distributions, LTT=0, LI=1; 2) Legendre expansion coefficients, LTT=1;

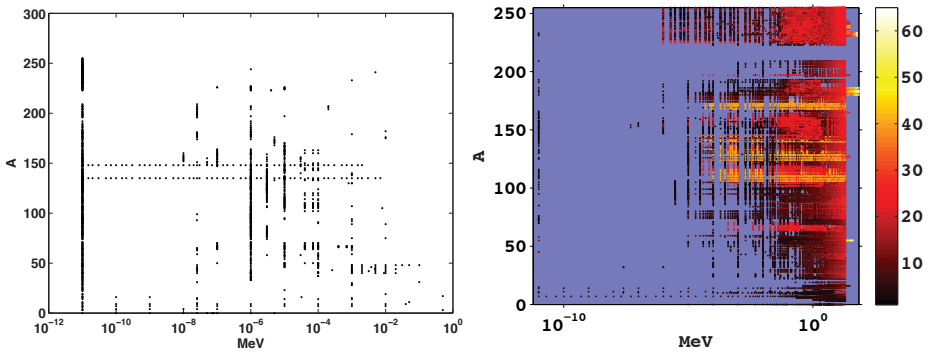

Fig. 3: A-E combinations where MF=4 MT=2 distribution are given as isotropic (left), or in Legendre representation (right) in ENDF/B-VII.1 and JENDL-4.0. Colour scales from low (dark) to high (bright) Legendre orders.

3) tabulated probabilities, LTT=2. Data storage demands understandably increases in this order. An additional factor is data availability. For instance, 74 materials were given as purely isotropic in JEFF-3.1.1 (2009), whereas no parallels could be found in the more recently released JENDL-4.0 and ENDF/B-VII.1. This does not necessarily negate the use of JEFF-3.1.1, since it contains materials and/or energy ranges still absent in the latter two libraries.

Fig. 3 summarizes the mass-energy (A-E) combinations where angular distribution is given as isotropic and that given in Legendre representation. Note that interpolation does not apply; the absence of a point indicates the absence of data rather than the continuity of data.

The first Legendre coefficient is of special interest because it allows the calculation of average energy loss. Its bi-variate A-E variation (Fig. 4) suggests trends of parameterization potential. Univariate plots (Fig. 5) suggest a straight-forward sigmoid dependence in the form of

$$Y = a + \frac{b}{1 + e^{-\frac{X+c}{d}}} \tag{1}$$

with the energy scale in logarithmic form. The A-dependence, however, merits a closer scrutiny (Fig. 6). The A-dependence at different energies exhibits common peaks and valleys at A around 53, 85, 143 and 209. It is therefore foreseeable that the Legendre coefficients may be further condensed as parameterized functions of A and E.

References

[1] A. Ferrari, P. Sala, A. Fassò, and J. Ranft, "FLUKA: a Multi-Particle Transport Code," Tech. Rep. CERN-2005-10, INFN/TC_05/11, SLAC-R-773, CERN, INFN, SLAC, 2005.

[2] G. Battistoni, S. Muraro, P. Sala, F. Cerutti, A. Ferrari, S. Rősler, A. Fassò, and J. Ranft, "Proceedings of the Hadronic Shower Simulation Workshop 2006, Fermilab 6–8 September 2006," vol. 896, pp. 31–49, AIP Conference Proceedings, 2007.

[3] M. Herman and A. Trikov, "ENDF-6 Formats Manual," Tech. Rep. Doc ENDF-102, BNL-XXXXX-2009, Brookhaven National Laboratory, 2009.

[4] D. E. Cullen, "PREPRO 2010," Tech. Rep. IAEA-NDS-39, IAEA, 2010.

[5] R. E. MacFarlane and A. C. Kahler, "Methods for Processing ENDF/B-VII with NJOY," *Nuclear Data Sheets*, vol. 111, pp. 2739–2889, DEC 2010.

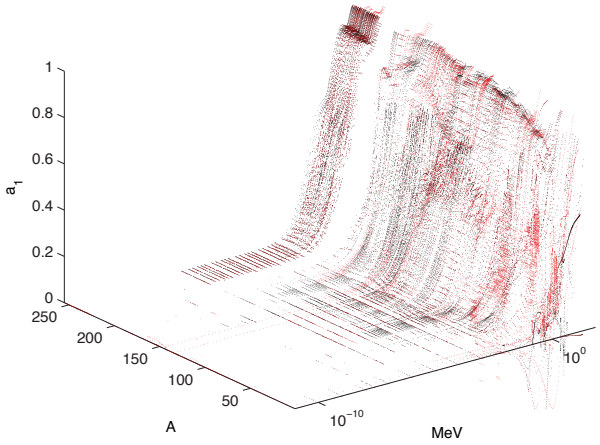

Fig. 4: The first Legendre coefficient given for MF=4 MT=2 by ENDF/B-VII.1 (red) and JENDL-4.0 (blue) as a function of A and E.

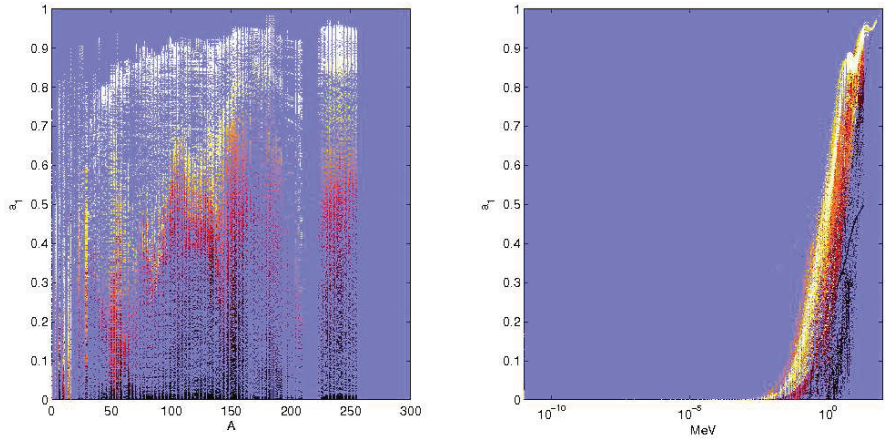

Fig. 5: The first Legendre coefficient given for MF=4 MT=2 by ENDF/B-VII.1 and JENDL-4.0. Left: variation with A, colour scales from low energy (dark) to high energy (bright). Right: variation with E, colour scales from low A (dark) to high A (bright).

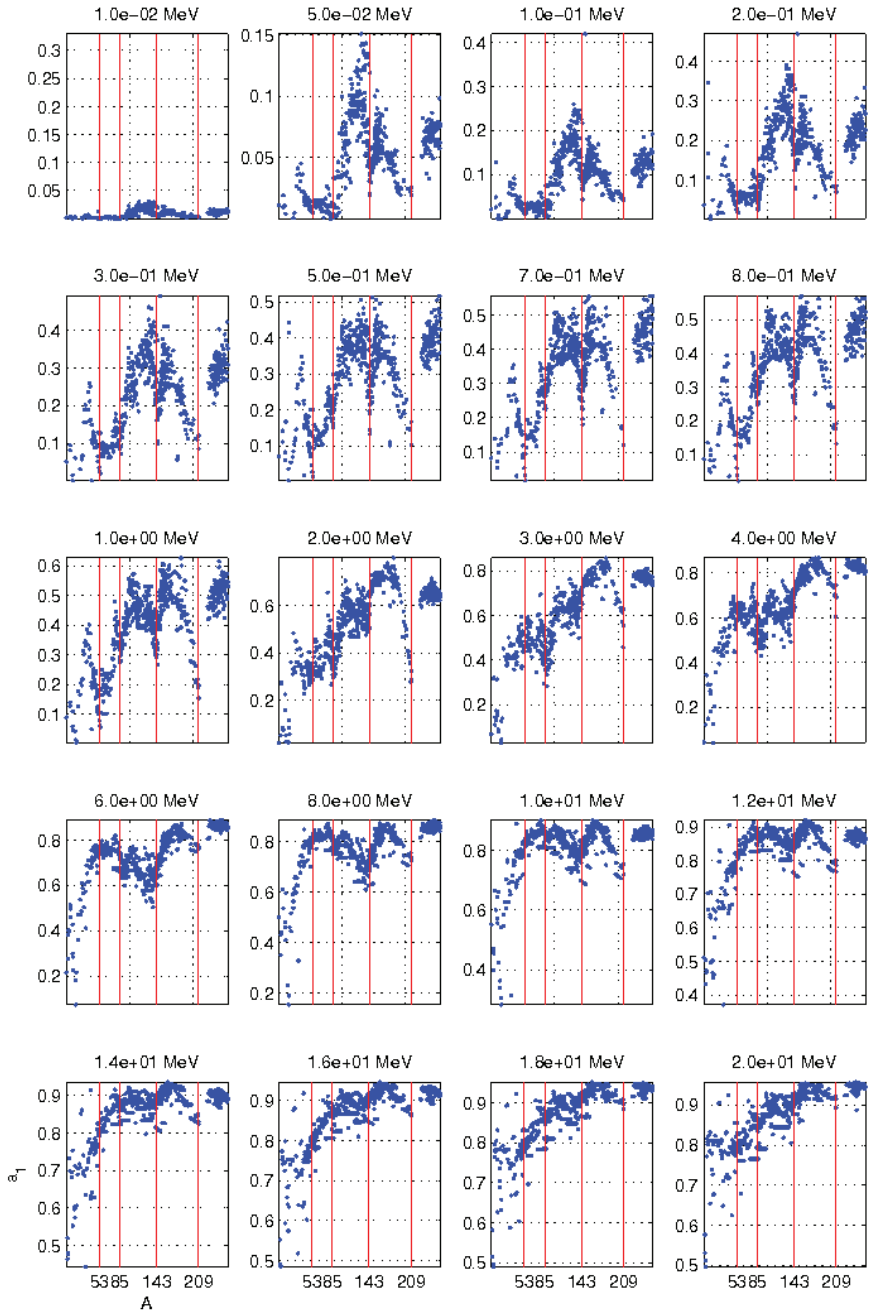

Fig. 6: Variation of the first Legendre coefficient with A, plotted at selected energies between 10 keV and 20 MeV. All subplots have been overlayed with lines A=53, 85, 143 and 209.